RESEARCH ARTICLE   **Open Access**

Changes in extremely heavy and light snow-cover winters due to global warming over high mountainous areas in central Japan

Hiroaki Kawase[1]*, Takeshi Yamazaki[2], Shiori Sugimoto[3], Takahiro Sasai[2], Rui Ito[4], Takashi Hamada[5], Masatoshi Kuribayashi[5], Mikiko Fujita[3], Akihiko Murata[1], Masaya Nosaka[1] and Hidetaka Sasaki[1]

Abstract

To investigate future changes in snow cover and snowfall over mountainous areas in central Japan, we conducted regional climate projections using a high-resolution non-hydrostatic regional climate model (NHRCM) with 5 km and 1 km grid spacings. Boundary conditions are derived from the database for Policy Decision making for Future climate change (d4PDF) 20 km regional climate projections (d4PDF20). The d4PDF20 assumes two future climates when global mean surface air temperatures are approximately 2 K and 4 K warmer than in the preindustrial period. Experiments with 5 km grid spacing are conducted by NHRCM for 372 years in d4PDF20 in each climate. Experiments with 1 km grid spacing are performed focusing on 5 years with heavy, median, and light snow cover of mountainous areas in each climate. In the years with heavy snow cover in 2 K and 4 K warming climates, snowfall is enhanced from late December to February at more than 2000 m above sea level (mASL) in the northern parts of Japan's Northern Alps, resulting in heavy snow cover comparable to that in the present climate. Heavy daily snowfall remarkably increases due to global warming in the years with heavy snow cover. At low elevations below 500 mASL, snowfall decreases in all ranges of snowfall intensity in the 4 K warming climate, while the frequency of heavy daily snowfall increases in the 2 K warming climate. Precipitation is enhanced around the Japan-Sea Polar-airmass Convergence Zone and the mountainous area facing the Sea of Japan, resulting in strengthened heavy snowfall at high elevations where the winter mean temperature is approximately − 10 °C in the present climate. On the other hand, remarkable reductions in snow cover and snowfall are projected in years with light snow cover. Our results indicate that global warming causes heavy and light mid-winter snowfalls at high elevations of Japan's Northern Alps that are more extreme than those in the present climate.

Keywords: Mountainous snow cover, Heavy snowfall, Regional climate modeling, Global warming, Dynamical downscaling, Japan's Northern Alps
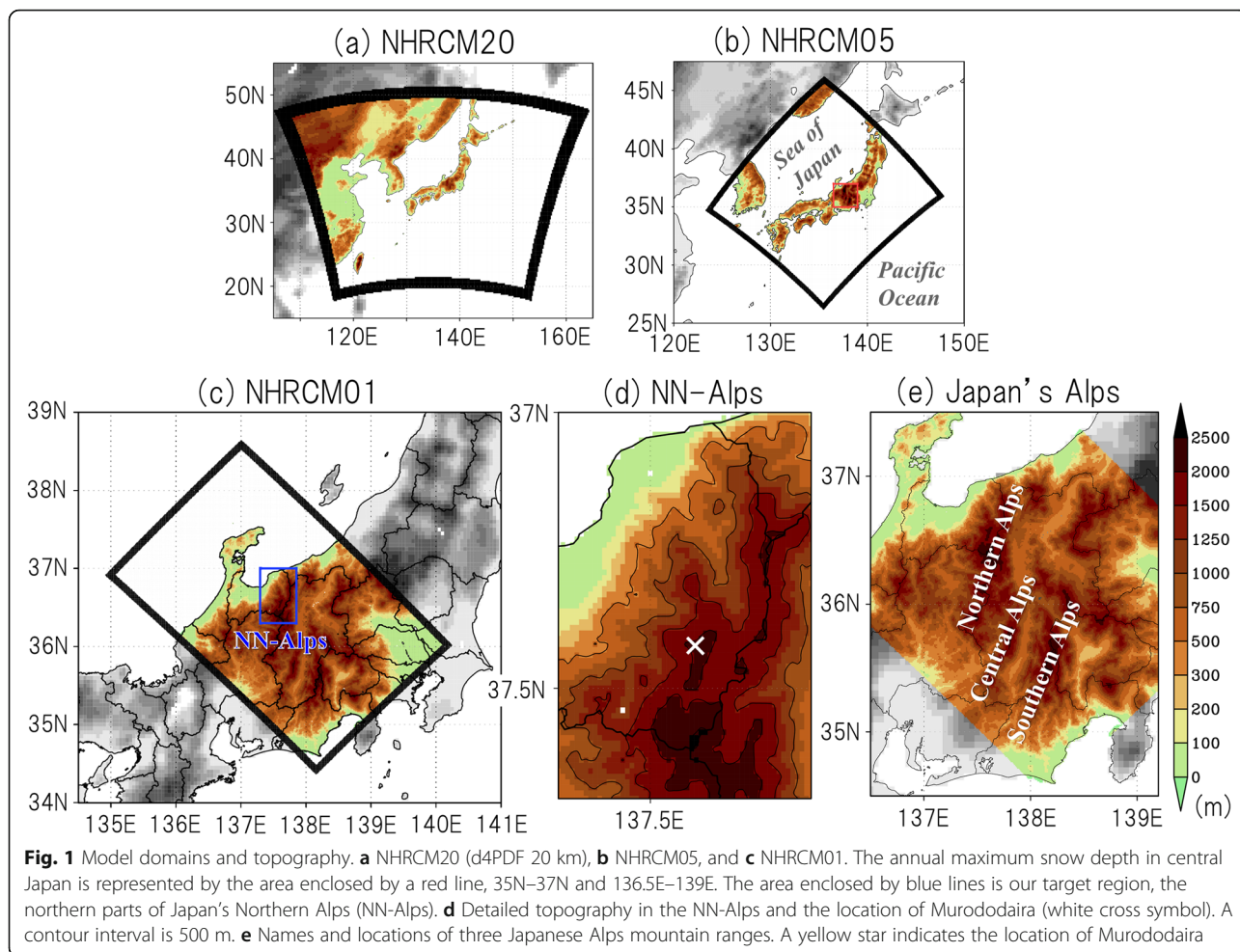
Introduction

Japan's Northern Alps, located in central Japan, are known as one of the deepest snow-cover regions in the world (Fig. 1). The cold and dry northwesterly from the Eurasian continent, called the East Asian Winter Monsoon, obtains plenty of moisture from the relatively warm Sea of Japan, causing snowfall over the Sea of Japan's coast. Additionally, the topographic updraft enhances the snowfall over Japan's Northern Alps facing the Sea of Japan. In Japan's Northern Alps, at Murododaira (Fig. 1d), whose altitude is 2450 m above sea level (mASL), the snow depth and snow water equivalent (SWE) are about 600 cm and 3000 mm, respectively, in early spring (Aoki and Watanabe 2009; Kawase et al. 2015, 2018b, 2019a). Enormous SWEs in the mountainous areas are available as water resources in the spring and early summer in Japan.

* Correspondence: hkawase@mri-jma.go.jp
[1]Meteorological Research Institute, Japan Meteorological Agency, 1-1 Nagamine, Tsukuba 305-0052, Japan
Full list of author information is available at the end of the article

Fig. 1 Model domains and topography. **a** NHRCM20 (d4PDF 20 km), **b** NHRCM05, and **c** NHRCM01. The annual maximum snow depth in central Japan is represented by the area enclosed by a red line, 35N–37N and 136.5E–139E. The area enclosed by blue lines is our target region, the northern parts of Japan's Northern Alps (NN-Alps). **d** Detailed topography in the NN-Alps and the location of Murododaira (white cross symbol). A contour interval is 500 m. **e** Names and locations of three Japanese Alps mountain ranges. A yellow star indicates the location of Murododaira

Since the late 1980s, snow cover has been decreasing over the Japanese archipelago, especially in the central and western parts of Japan. Rapid warming changes snowfall to rainfall, resulting in a decrease in snow cover at low elevations (Ishizaka 2004; Suzuki 2006; Ishii and Suzuki 2011; Kawase et al. 2012). On the other hand, such reductions in snow cover are not observed in high mountainous areas where the annual variation of snow cover correlates with that of total precipitation (Suzuki 2006; Matsuura et al. 2005; Ishii and Suzuki 2011). Yamaguchi et al. (2011) pointed out that snow cover is sensitive to air temperature at low elevations, while it is influenced by precipitation rather than air temperature at high elevations. Kawase et al. (2018b) simulated annual variations of snow depth around Japan's Northern Alps and showed that annual variations of snow cover depend on elevation.

Global climate models project that snow cover will decrease due to global warming in most parts of the world, while snow cover could increase in very cold regions where the winter mean temperature is lower than − 20 °C in the present climate (Raisanen 2007; Brown and Mote 2009). Basically, global climate models cannot resolve complex terrain because of the horizontal resolutions (~ 150 km). Snow-cover distributions in mountainous areas are, however, strongly influenced by complex terrain. Dynamical downscaling using a regional climate model (RCM) is a useful method of reproducing and projecting snow cover in mountainous areas. For instance, an RCM with a horizontal grid spacing of less than 2 km is required to calculate snow cover over the Rocky Mountains (Ikeda et al. 2010; Rasmussen et al. 2011; Gutmann et al. 2012). Rasmussen et al. (2011) conducted pseudo-global warming downscaling (Kimura and Kitoh 2007) and evaluated future changes in snow cover over the Rocky Mountains using the Weather Research and Forecasting (WRF) model. They indicated that global warming enhanced melting at lower elevations and increased snowfall at higher elevations. Rasmussen et al. (2014) indicated that snowpack did not change until January over the Colorado Headwaters in the future climate, while, above 3000 mASL, snowpack increased from January to March and decreased after April. On the other hand, an enhancement of heavy

snowfall has been projected around the Great Lakes because the lake ice would melt due to global warming, and much water vapor could evaporate from the lakes (Gula and Peltier 2012; Notaro et al. 2015). Steger et al. (2012) pointed out that, over the European Alps, the SWE would largely decrease at the lower elevations, while the changes in the SWE were small at the higher elevations. These changes are consistent with the snow cover changes in the Colorado Headwaters (Rasmussen et al. 2011, 2014). Steger et al. (2012) also stated that future changes in snow cover over the European Alps had inter-model variability.

In Japan, some studies have indicated that the maximum snow depth and SWE would decrease due to global warming (Hara et al. 2008; Inoue and Yokoyama 1998, 2003; Kawase et al. 2013, 2016). Additionally, an East Asian Winter Monsoon weakened due to global warming (Hori and Ueda 2006; Kawase et al. 2015) decreases winter precipitation, including snowfall, on the Sea of Japan side. Katsuyama et al. (2017) also showed that global warming would decrease the snow depth in Hokkaido, a northern part of Japan, throughout the winter season and discussed future changes in the seasonal variation of snowpack types, such as melt forms and depth hoar. Kawase et al. (2016) analyzed the database for Policy Decision making for Future climate change (hereafter referred to as d4PDF) (Mizuta et al. 2017) and pointed out that extremely heavy daily snowfall could increase in inland areas over the Sea of Japan side in central Japan due to global warming. They stated that enhancements of the Japan-Sea Polar-airmass Convergence Zone (hereafter referred to as the JPCZ) and topographic updraft brought about heavier snowfall over inland areas where the air temperature will still be lower than 0 °C in the future climate.

The d4PDF, which contains a global climate simulation with about 60 km grid spacing and a regional climate simulation with 20 km grid spacing (hereafter referred to as d4PDF20), is a useful dataset for evaluating the impact of global warming on extreme events, such as heat waves (Imada et al. 2019), heavy rainfalls (Kawase et al. 2019b; Ohba and Sugimoto 2019), and heavy snowfalls (Kawase et al. 2016). However, d4PDF20 has insufficient grid spacing to resolve the complex mountains of Japan. Kawase et al. (2018a) conducted dynamical downscaling from several ensemble experiments in the d4PDF20 in the present climate using the non-hydrostatic regional climate model (NHRCM) (Sasaki et al. 2008) with 5 km grid spacing (hereafter referred to as the 5km_HIST experiment). Based on the 5km_HIST experiment, they clarified that the geographical boundaries of extremely heavy snowfall events caused by two typical patterns—a cold air outbreak and an extratropical cyclone—are more clearly defined than those of other

snowfall events. As with Kawase et al. (2018a), Sasai et al. (2019) conducted dynamical downscaling from d4PDF20 in two future climates, assuming that the global mean temperatures are 2 K and 4 K warmer than those in the pre-industrial period (Mizuta et al. 2017; Fujita et al. 2019) (hereafter referred to as the 5km_2K and 5km_4K experiments, respectively). For 5km_2K and 5km_4K experiments, they selected two ensemble members from each sea surface temperature (SST) pattern in d4PDF, which has six SST patterns, and conducted a 31-year simulation for each ensemble member. Then, a 372-year simulation was obtained in each future climate as with the present climate (Kawase et al. 2018a).

Over Japan's Northern Alps, the snow depth is, however, overestimated by the NHRCM with 5 km grid spacing (hereafter referred to as NHRCM05), especially around 1000–2000 mASL, as compared with snow observations and the NHRCM with 2 km grid spacing (hereafter referred to as NHRCM02) (Kawase et al. 2019a). NHRCM05 cannot resolve small-scale convective precipitation over the Sea of Japan, which results in the overestimation of snow depth on the windward side of Japan's Northern Alps. Therefore, at least 2 km grid spacing is required to accurately simulate and project the snow cover over the complex mountains of central Japan, such as Japan's Northern Alps.

Most previous studies focus on the climatological changes in snow cover due to global warming (Hara et al. 2008; Inoue and Yokoyama 2003; Kawase et al. 2016), and the horizontal resolution of the regional climate model is coarser than 5 km, which is not high enough to simulate winter precipitation in the mountainous areas of central Japan, as pointed out by Kawase et al. (2019a). The purpose of this study is to evaluate the impact of global warming on snowfall and snow cover in the high mountainous areas of central Japan in extremely heavy and light snow-cover years using the NHRCM with 1 km grid spacing (hereafter referred to as NHRCM01).

Methods/Experimental
Experimental designs
Regional mean maximum snow depths are calculated in the mountainous areas of central Japan, where the altitude is higher than 1000 mASL (red frame in Fig. 1b) in the 5km_HIST, 5km_2K, and 5km_4K experiments. Five years of heaviest, median, and lightest snow cover (hereafter referred to as heavy snow-cover years, median snow-cover years, and light snow-cover years, respectively) are selected from each climate (Table 1). Focusing on three types of winter, dynamical downscaling is conducted by using the NHRCM with 1 km grid spacing (hereafter referred to as NHRM01) from the 5km_HIST,

Table 1 Selected ensemble members and the regional mean annual maximum snow depth

Historical (HPB)	Year	Snow depth (cm)	2 K warming (HFB_2K)	Year	Snow depth (cm)	4 K warming (HFB_4K)	Year	Snow depth (cm)
Light snow-cover year								
m004	2009	118.8	CC_m105	2061	92.8	CC_m101	2095	52.4
m004	2000	131.3	CC_m105	2084	92.9	HA_m105	2081	54.6
m022	2004	132.7	MP_m105	2086	94.6	GF_m105	2081	58.3
m005	2010	138.2	CC_m105	2080	95.6	CC_m101	2101	64.9
m002	1995	143.0	MP_m105	2061	104.8	MI_m101	2087	69.7
Median snow-cover year								
m002	1984	209.7	MP_m105	2063	171.5	MR_m101	2097	137.6
m008	2006	209.8	HA_m105	2069	171.8	CC_m105	2107	137.8
m010	2000	209.8	HA_m105	2077	172.2	MI_m101	2097	138.2
m021	1981	210.0	MI_m101	2064	172.3	HA_m101	2084	139.0
m022	1985	210.4	GF_m101	2064	172.5	GF_m101	2106	139.0
Heavy snow-cover year								
m004	1992	285.3	GF_m105	2069	259.1	GF_m101	2108	219.6
m009	1982	296.3	GF_m101	2070	259.7	MP_m101	2103	223.5
m004	2010	298.9	CC_m101	2072	274.4	MI_m105	2096	231.4
m008	1989	300.6	MI_m105	2076	275.0	GF_m101	2091	231.5
m004	1981	317.1	GF_m101	2076	285.4	GF_m101	2100	243.8

5km_2K, and 5km_4K experiments, which are referred to as the 1km_HIST, 1km_2K, and 1km_4K experiments, respectively. The experimental designs are summarized in Table 2.

Figure 1a–c shows the model domains and topography resolved by NHRCM20, NHRCM05, and NHRCM01, respectively. NHRCM01 resolves complex mountains in central Japan (Fig. 1c, d). Numerical experiments were conducted from August 20 to August 29 in the following year to simulate the annual snow cover of central Japan's high elevations. The precipitation process was calculated only by a microphysics scheme (Ikawa et al. 1991) in NHRCM01, while NHRCM05 used both the microphysics scheme and Kain-Fritsch cumulus convective parameterization (Kain and Fritsch 1993). The atmospheric boundary layer process was calculated by the improved Mellor-Yamada-Nakanishi-Niino (MYNN) level 3 (Nakanishi

and Niino 2004). The land-surface process was calculated by the improved MRI/JMA Simple Biosphere (iSiB), which was updated from that used by Hirai and Oh'izumi (2004). An urban canopy model (Aoyagi and Seino 2011; Ito et al. 2018) was used in NHRCM01, as with NHRCM05. The other physical parameterizations and the experimental design in NHRCM01 are summarized in Tables 3 and 4, respectively.

Results and discussion

Mean maximum snow cover in the 2 K and 4 K warming climates

Figure 2a and b shows horizontal distributions of 15-year mean annual maximum snow cover, which consists of five light, five median, and five heavy snow-cover years, simulated by the 5km_HIST and 1km_HIST experiments, respectively. Snow cover simulated by the 5km_HIST experiment exceeds 900 cm over

Table 2 Experimental design

Experimental name	Climate	Total year	Detailed description
5km_HIST	Present climate	372	31 years and 12 ensemble experiments
5km_2K	Future climate (+2 K)	372	31 years and 2 ensemble experiments in 6 SST patterns
5km_4K	Future climate (+4 K)	372	
1km_HIST	Present climate	15	5 heaviest snow years in 372 years
1km_2K	Future climate (+ 2K)	15	5 median snow years in 372 years
1km_4K	Future climate (+4 K)	15	5 lightest snow years in 372 years

Table 3 Specifications of the NHRCM01

Specification	Detail
Numerical model	Non-hydrostatic Regional Climate Model (Sasaki et al. 2008)
Horizontal resolution	1 km
Boundary condition	d4PDF05 (Kawase et al. 2018a; Sasai et al. 2019)
Nesting	One-way nesting
Nudging	Spectral nudging (Nakano et al. 2012)
Initial date	August 20

the northern side of Japan's Northern Alps facing the Sea of Japan (Fig. 2a). On the other hand, the 1km_HIST experiment simulates snow cover of 700 cm over the high elevations above 2000 mASL at the northern part of Japan's Northern Alps, which is consistent with the snow-cover survey at Murododaira in Japan's Northern Alps (Aoki and Watanabe 2009; Kawase et al. 2019a). NHRCM01 can resolve a steep valley, called the Kurobe Gorge. Deep snow-cover areas are limited over the high mountainous areas. The overestimation of snow cover in the 5km_HIST experiment is caused by the envelope-type high mountains (Kawase et al. 2018a) and a lack of horizontal resolution for calculating the small-scale convections over the Sea of Japan (Kawase et al. 2019a).

Figure 2c–f shows future changes in the 15-year mean annual maximum snow cover projected by the 1km_2K and 1km_4K experiments. Both simulations indicate that the annual maximum snow cover will decrease due to global warming over whole areas. The 1km_4K experiment projects more than a 150 cm decrease in the maximum snow cover above 1000 mASL in Japan's Northern Alps (Fig. 2d). The decrease in snow cover is larger at high elevations than at low elevations (Fig. 2c, d), while the decreasing ratio is larger at low elevations than at high elevations (Fig. 2e, f), which is consistent with the findings of previous studies (Hara et al. 2008; Kawase et al. 2013). Here, we focus on the northern part of Japan's Northern Alps (hereafter, NN-Alps; the blue rectangle in Fig. 1c), where the complex topography is well resolved by the NHRCM01 (Fig. 1d), and the enormous snow cover is calculated in our model domain.

We individually analyze the snow cover changes in three types of winter.

Seasonal variations of snow cover and snowfall

Seasonal variations of snow cover in the 1km_HIST experiment are different among three types of winter at elevations above 2000 mASL of the NN-Alps (Fig. 3a). In heavy snow-cover years, peak snow cover appears in late March to early April, and snow cover decreases after mid-April. On the other hand, peak snow cover appears in mid-March and late February in median and light snow-cover years, respectively. The seasonal variation of snow cover in light snow-cover years shows a gentle slope as compared with the others.

Figure 3b–d shows future changes in seasonal variations of snow cover above 2000 mASL of the NN-Alps. In heavy snow-cover years, the seasonal variation in the 1km_2K experiment is similar to that in the 1km_HIST experiment from December to mid-March (Fig. 3b). After late March, the snow cover gradually decreases in the 1km_2K experiment, which is approximately half a month earlier than in the 1km_HIST experiment. From October to January, snow cover in the 1km_4K experiment is much smaller than that in the 1km_HIST experiment, while the differences become smaller as winter progresses. In mid-February, the 5-year mean snow cover in the 1km_4K experiment is comparable to that in the 1km_HIST experiment. After mid-February, the 1km_4K experiment shows a long continuous peak of snow cover until early April. Snow cover rapidly decreases after mid-April, as with the 1km_HIST and

Table 4 Physical processes in the NHRCM01

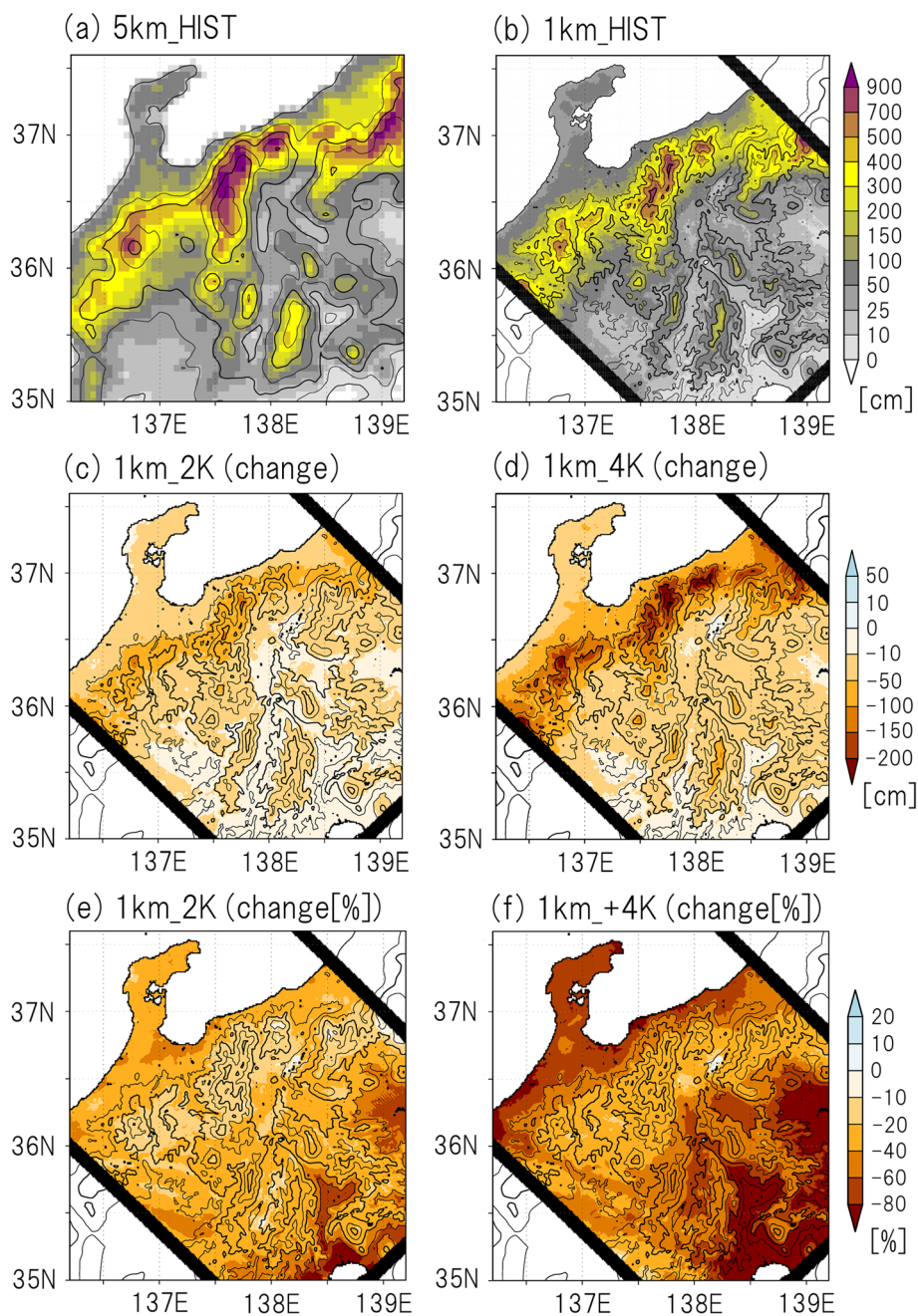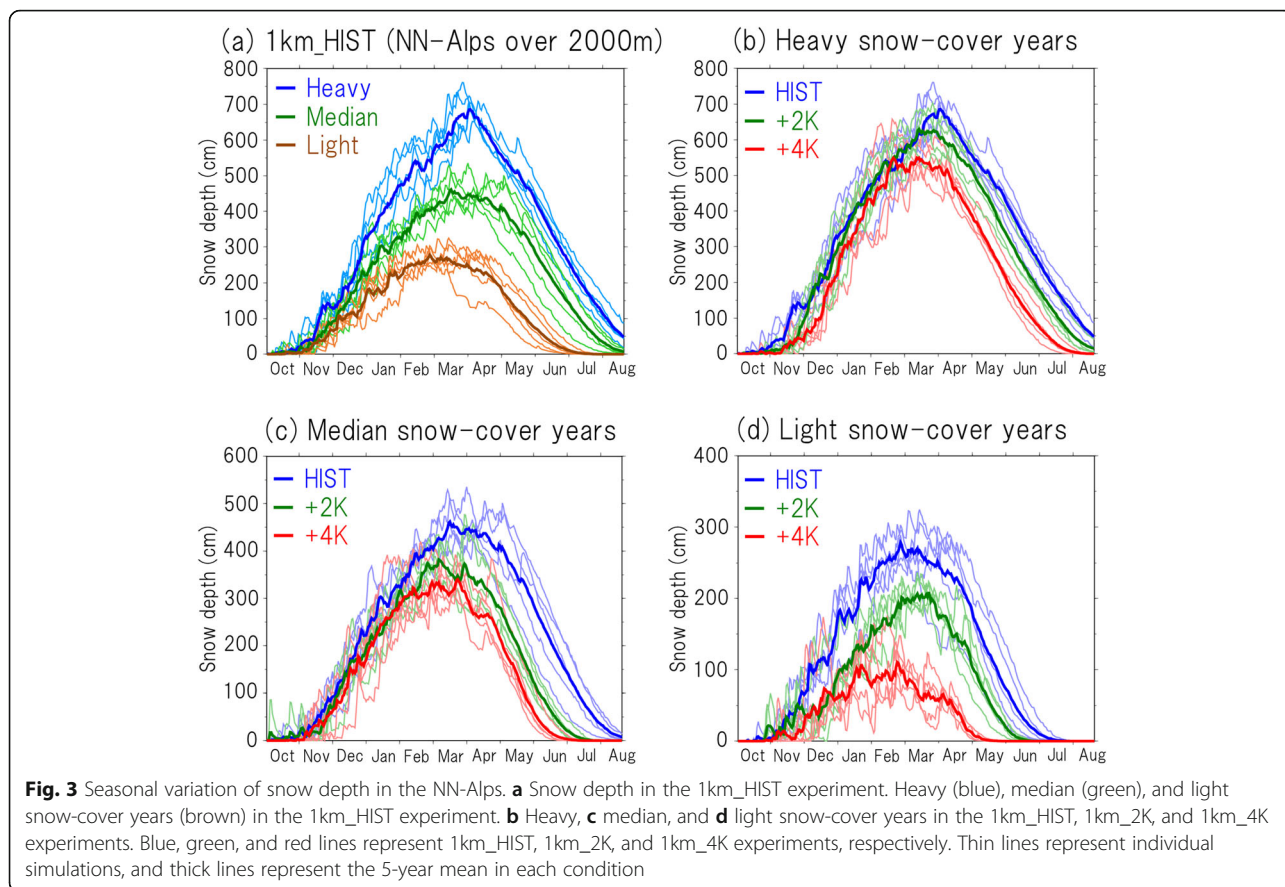| Process	Physical parameterization
Microphysics	Bulk-type cloud microphysics (Ikawa et al. 1991)
Radiation process	Clear-sky radiation scheme (Yabu et al. 2005) Cloud radiation scheme (Kitagawa 2000)
Boundary-layer process	Improved Mellor-Yamada-Nakanishi-Niino (MYNN) Level 3 (Nakanishi and Niino 2004)
Land-surface process	Improved MRI/JMA Simple Biosphere (iSiB) (Hirai and Oh'izumi 2004)
Urban model	Square Prism Urban Canopy Scheme (SPUC) with snow cover process (Aoyagi and Seino 2011; Ito et al. 2018)

Fig. 2 Horizontal distribution of the 15-year mean annual maximum snow depth and changes due to global warming. Fifteen-year mean maximum snow depth simulated by **a** 5km_HIST and **b** 1km_HIST experiments. Differences in maximum snow depths between **c** 1km_2K and 1km_HIST experiments and **d** 1km_4K and 1km_HIST experiments. Contours represent elevations. The contour interval is 500 m, and the thick contour interval is 1000 m

1km_2K experiments, and snow cover disappears in late July. The shapes of the seasonal variations in the 1km_HIST, 1km_2K, and 1km_4K experiments are different.

In median snow-cover years, snow covers simulated by the 1km_2K and 1km_4K experiments are less than that simulated by the 1km_HIST experiment, except in December (Fig. 3b). The half-monthly snowfalls in the

1km_2K and 1km_4K experiments are comparable to or larger than the snowfall in the 1km_HIST experiment from December to January (figure not shown), resulting in similar snow depths among the three climates. As compared with the heavy snow-cover years, the 1km_2K experiment is similar to the 1km_4K experiment. In the light snow-cover years, the snow cover in the 1km_4K

Fig. 3 Seasonal variation of snow depth in the NN-Alps. **a** Snow depth in the 1km_HIST experiment. Heavy (blue), median (green), and light snow-cover years (brown) in the 1km_HIST experiment. **b** Heavy, **c** median, and **d** light snow-cover years in the 1km_HIST, 1km_2K, and 1km_4K experiments. Blue, green, and red lines represent 1km_HIST, 1km_2K, and 1km_4K experiments, respectively. Thin lines represent individual simulations, and thick lines represent the 5-year mean in each condition

experiment is much less than that in the 1km_HIST experiment for the entire duration of snow cover, except for December of one year (Fig. 3d). The 5-year mean maximum snow depth is approximately 100 cm in the 1km_4K experiment, which is about one-third of the maximum snow depth in the 1km_HIST experiment. The snow cover disappears by mid-May in the 1km_4K experiment, which is approximately 2 months earlier than that in the 1km_HIST experiment. Therefore, the impact of global warming on the seasonal variation of snow cover depends on the type of winter. Snow cover is clearly reduced in the light snow-cover years as compared to that of heavy snow-cover years. This indicates that, with the progress of global warming, the amplitude of the interannual variation in mid-winter snow cover would become larger than that in the present climate. On the other hand, global warming reduces the snow cover during snow-melting periods in both heavy and light snow-cover years. Note that selected 5-year simulations are conducted for each type of winter.

Figure 4 shows the time sequences of half-monthly accumulated snowfall, rainfall, and precipitation simulated by the 1km_HIST, 1km_2K, and 1km_4K experiments, respectively, in heavy and light snow-cover years. From October to November, the 1km_

HIST experiment simulates the largest amounts of snowfall in both heavy and light snow-cover years. In heavy snow-cover years, it is noteworthy that, among the three experiments, the 1km_4K experiment calculates the largest snowfall from the latter half of December to the first half of February. The amount of snowfall in the 1km_2K experiment also exceeds that in the 1km_HIST experiment from January to February. In heavy snow-cover years, global warming can bring more snowfall in mid-winter than in the present climate, resulting in plenty of snow cover comparable to that of the present climate in February (Fig. 3b). In light snow-cover years, snowfall considerably decreases in the 1km_4K experiment during the entire cold season (Fig. 4b). From the latter half of January to March, the 1km_2K experiment simulates larger snowfalls than does the 1km_HIST experiment.

In heavy snow-cover years, all simulations show little rainfall in winter (December to February: DJF), while the 1km_4K experiment simulates increased rainfall in autumn and spring (Fig. 4c). In light snow-cover years, the 1km_2K and 1km_4K experiments show increased rainfall during mid-winter (Fig. 4d). The amount of half-monthly rainfall is above 50 mm from January to
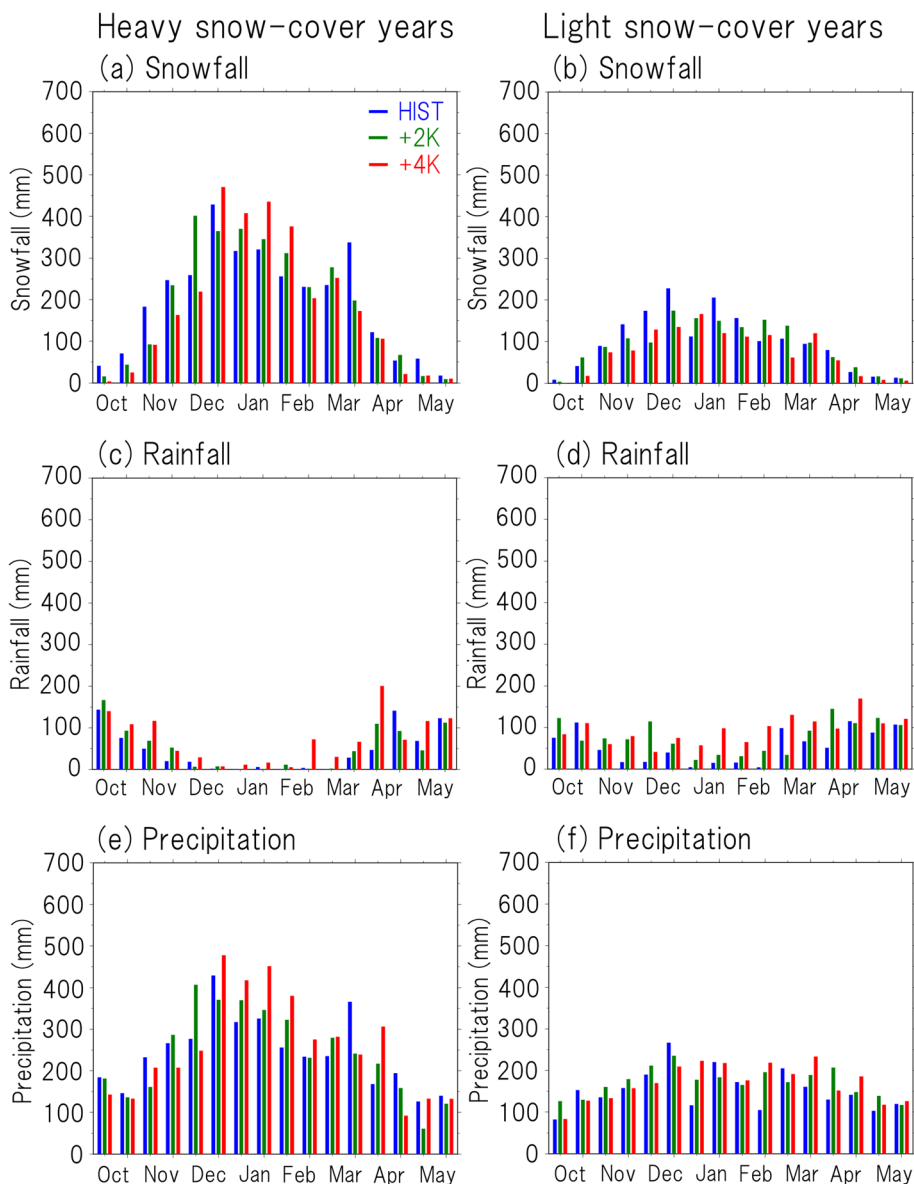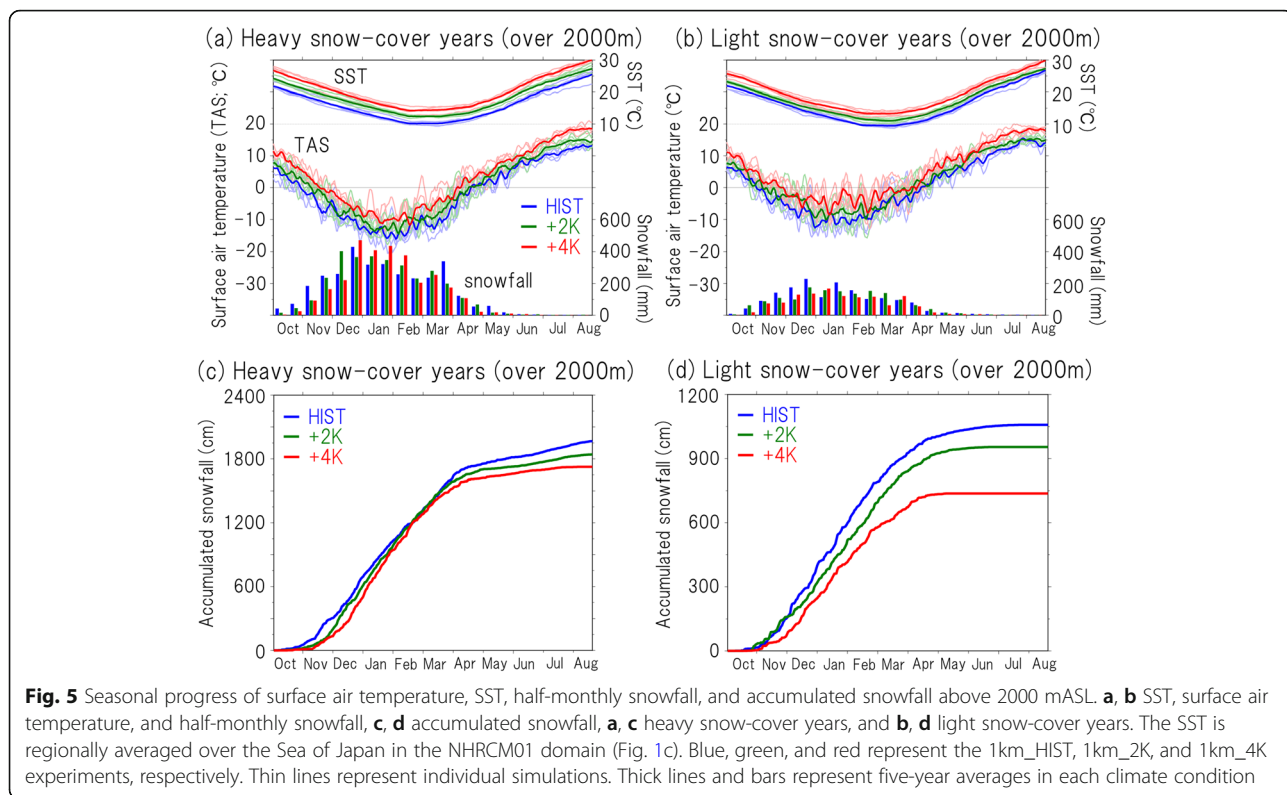
Fig. 4 Seasonal variations in snowfall, rainfall, and precipitation above 2000 mASL of the NN-Alps. Snowfall includes graupel, and precipitation is the sum of snowfall and rainfall. **a** Snowfall in heavy snow-cover years, **b** snowfall in light snow-cover years, **c** rainfall in heavy snow-cover years, **d** rainfall in light snow-cover years, **e** precipitation in heavy snow-cover years, and **f** precipitation in light snow-cover years. Blue, green, and red represent the 1km_HIST, 1km_2K, and 1km_4K experiments, respectively. Thin lines represent individual simulations, and bars represent five-year averages in each climate condition

February in the 1km_4K experiment. The total precipitation shows changes similar to those of the snowfall in heavy snow-cover years (Fig. 4e), indicating that the increased precipitation during mid-winter results in increased snowfall above 2000 mASL of the NN-Alps. Heavy and light snow-cover years also show an increase in total precipitation in January and February (Fig. 4f). However, snowfall decreases in light snow-cover years since rainfall increases due to warming (Fig. 4d).
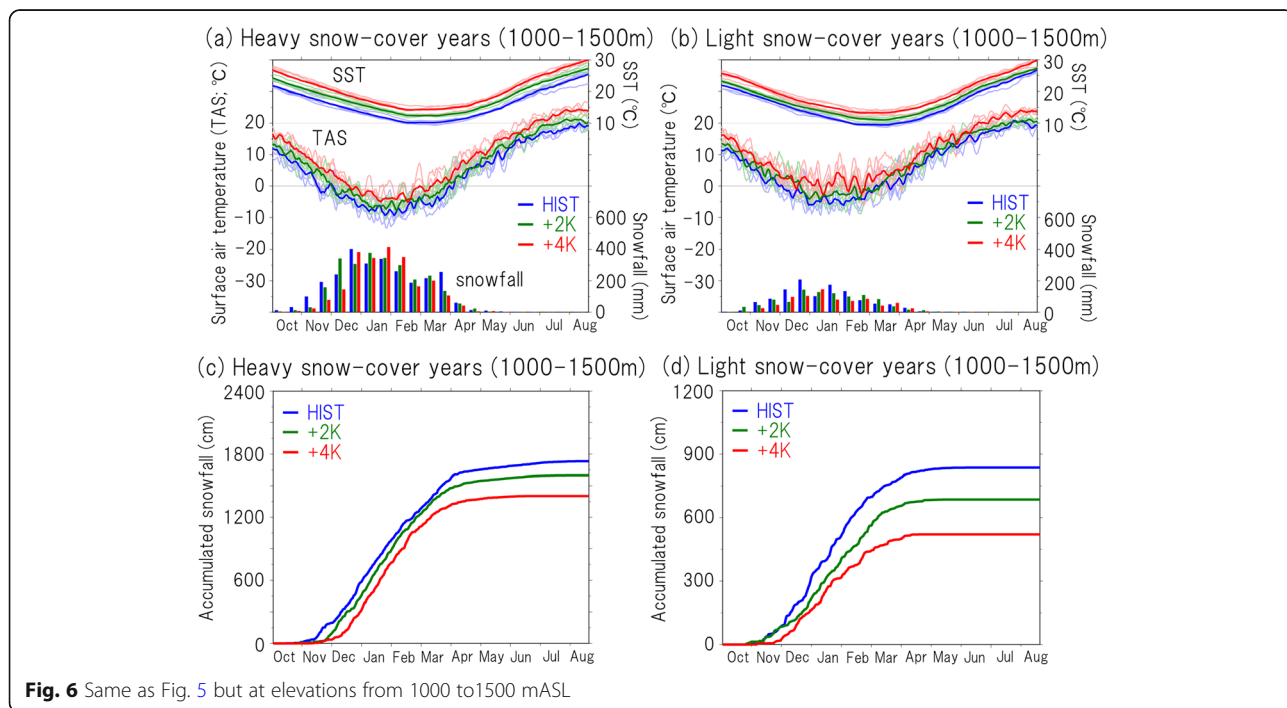
Seasonal variations of snowfall at high and middle elevations

Snowfall over Japan's Northern Alps is strongly influenced by the air temperature and SST of the Sea of Japan. Figures 5 and 6 show the seasonal variations of the daily mean SST, surface air temperature, and half-monthly accumulated snowfall, which are the same as in Fig. 4a, b, over 2000 mASL and 1000 to 1500 mASL of the NN-Alps. Here, the SST is regionally averaged over

Fig. 5 Seasonal progress of surface air temperature, SST, half-monthly snowfall, and accumulated snowfall above 2000 mASL. **a**, **b** SST, surface air temperature, and half-monthly snowfall, **c**, **d** accumulated snowfall, **a**, **c** heavy snow-cover years, and **b**, **d** light snow-cover years. The SST is regionally averaged over the Sea of Japan in the NHRCM01 domain (Fig. 1c). Blue, green, and red represent the 1km_HIST, 1km_2K, and 1km_4K experiments, respectively. Thin lines represent individual simulations. Thick lines and bars represent five-year averages in each climate condition

the Sea of Japan in the NHRCM01 domain (Fig. 1c). Above 2000 mASL of the NN-Alps, the 5-year mean surface air temperature is lower than − 10 °C from mid-December to mid-March in the 1km_HIST experiment (Fig. 5a). In the 1km_4K experiment during the same

term, the surface air temperature is still lower than − 5 °C, which is cold enough to snow. No year shows positive surface air temperature from December to mid-February. The SST in the 1km_4K experiment exceeds 15 °C from December to January, which is approximately

Fig. 6 Same as Fig. 5 but at elevations from 1000 to 1500 mASL

5 °C higher than that in 1km_HIST. The warmer SST results in more moisture evaporating from the Sea of Japan and larger amounts of snowfall below freezing temperatures. Note that SSTs are given in our simulation. SSTs are not influenced by short-term variations in atmospheric conditions. On the other hand, the mean surface air temperature is between 0 and − 5 °C in the 1km_4K experiment, and some years occasionally exceed 0 °C above 2000 mASL of the NN-Alps in mid-winter in light snow-cover years (Fig. 5b), which causes rainfall even in mid-winter (Fig. 4d). We will discuss the influence of the basic air temperature on the total snowfall in each type of winter in a later section. Daily variations of the surface air temperature are larger in light snow-cover years than those in heavy snow-cover years, which implies that extra-tropical cyclones pass more frequently in light snow-cover years. Warm and cold air advections occur before and after the passing of the extratropical cyclone, respectively.

At 1000–1500 mASL of the NN-Alps, snowfall dramatically decreases in the 1km_4K experiment from November to the first half of December, when the surface air temperature exceeds 0 °C, in heavy snow-cover years (Fig. 6a). The snowfall in the 1km_4K experiment is comparable to or larger than that in the 1km_HIST experiment from the latter half of December to the first half of March. In light snow-cover years, the surface air temperature in the 1km_HIST and 1km_2K experiments is lower than 0 °C from December to February, while the surface air temperature frequently exceeds 0 °C in the 1km_4K experiment, and snowfall decreases through most of the winter (Fig. 6b). As with elevations above 2000 mASL in the NN-Alps, the daily variation of the surface air temperature in light snow-cover years is larger than that in heavy snow-cover years.
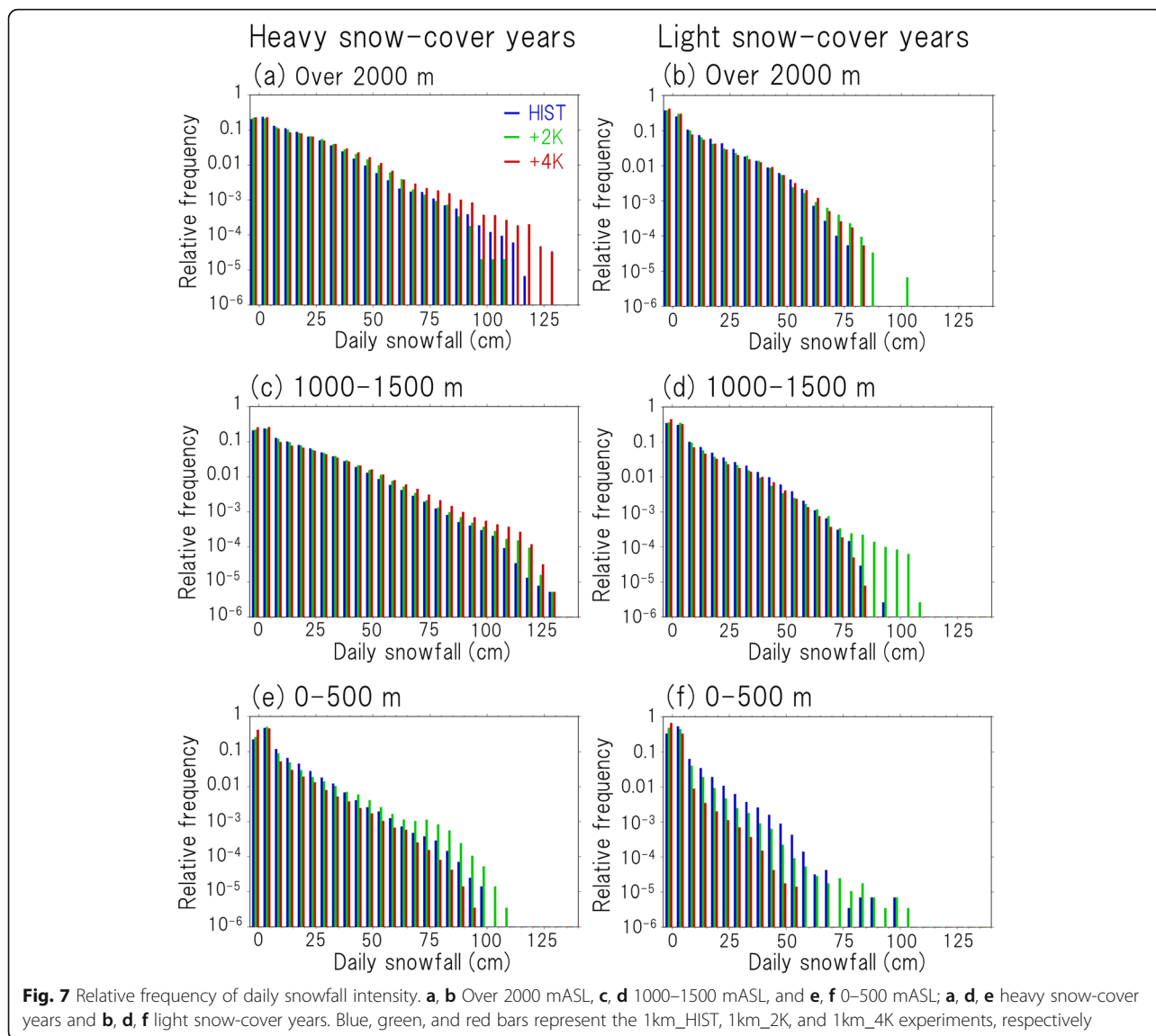
Accumulated snowfalls from October to August are shown in Figs. 5c, d and 6c, d. In heavy snow-cover years, the accumulated snowfalls in three climates are comparable from mid-February to mid-March (Fig. 5c), which results from considerable amounts of snowfall from late December to February (Fig. 4a). The differences in accumulated snowfall become larger after mid-March. In light snow-cover years, there is a large difference among the three climates, although there is a large 5-year variation in the 1km_4K experiment (Fig. 5d). Above 1000–1500 mASL of the NN-Alps, the accumulated snowfalls in the 1km_2K and 1km_4K experiments are lower than that in the 1km_HIST experiment, although some years overlap between the 1km_HIST and 1km_2K experiments (Fig. 6c). In light snow-cover years, the seasonal variations of accumulated snowfall are different among the three periods (Fig. 6d), which are similar to those above 2000 mASL of the NN-Alps (Fig. 5d).

Changes in daily snowfall intensity

Kawase et al. (2016) pointed out an enhancement of the extremely heavy daily snowfall, occurring once every 10 years, in inland areas over the Sea of Japan side of central Japan due to global warming. Figure 7 shows relative frequencies of daily snowfall intensity over three elevations, i.e., above 2000 mASL, 1000–1500 mASL, and 0–500 mASL of the NN-Alps. Here, the daily snowfall is accumulated by the increment of the hourly snow depth, which is consistent with the definition of the Japan Meteorological Agency. Above 2000 mASL, the number of non-snowfall days increases, and the number of weak daily snowfalls decreases due to global warming (Fig. 7a). Daily snowfall—more than 30 cm/day—occurs more frequently in the 1km_2K and 1km_4K experiments than in the 1km_HIST experiment. Extremely heavy daily snowfall—more than 80 cm/day—remarkably increases in the 1km_4K experiment. These results indicate that global warming enhances heavy daily snowfall and causes heavy daily snowfall not previously experienced above 2000 mASL in heavy snow-cover years. In light snow-cover years (Fig. 7b), the number of non-snowfall days increases, and the relative frequency decreases for most snowfall intensities. However, the frequency of heavy daily snowfalls—more than 60 cm/day—increases both in the 1km_2K and 1km_4K experiments, even in light snow-cover years.

Changes in the daily snowfall intensity above 1000–1500 mASL in heavy snow-cover years (Fig. 7c) are similar to those above 2000 mASL (Fig. 7a), while the frequency of daily snowfall increases over 50 cm/day due to global warming. In the 1km_4K experiment, extremely heavy snowfall occurs most frequently above 1000–1500 mASL, as with above 2000 mASL. In light snow-cover years, the daily snowfall frequency decreases in most ranges of snowfall intensity. Extremely heavy snowfall—more than 80 cm/day—however, occurs most frequently in 1km_2K.

Low elevations—below 500 mASL—show different changes in the frequency of daily snowfall intensity as compared with high elevations (Fig. 7e–f). In heavy snow-cover years, it is noteworthy that the 1km_2K experiment shows an increase in heavy snowfall—more than 40 cm/day—(Fig. 6e) while the daily snowfall frequency decreases in all ranges of snowfall intensity in 1km_4K. In light snow-cover years, daily snowfall frequency dramatically decreases at 0–500 mASL of the NN-Alps due to global warming (Fig. 6f). Note that three types of winter are defined using the annual maximum snow depth in central Japan exceeding 1000 mASL. In the next subsection, we will discuss changes in the winter total precipitation at each elevation around the NN-Alps in each type of winter.

Fig. 7 Relative frequency of daily snowfall intensity. **a**, **b** Over 2000 mASL, **c**, **d** 1000–1500 mASL, and **e**, **f** 0–500 mASL; **a**, **d**, **e** heavy snow-cover years and **b**, **d**, **f** light snow-cover years. Blue, green, and red bars represent the 1km_HIST, 1km_2K, and 1km_4K experiments, respectively

Relationship between mean air temperature and total precipitation during each winter

Takeuchi et al. (2008) investigated the relationship between the winter mean air temperature and precipitation in heavy-snowfall areas of Japan and identified a high negative correlation between the winter mean air temperature and precipitation, i.e., there was more precipitation with lower temperatures. As with Takeuchi et al. (2008), we investigated the relationship between the winter mean air temperature (hereafter referred to as the winter temperature) and the winter total precipitation (hereafter referred to as the winter precipitation) using our simulation results. Here, the winter is from December to February (DJF). Our experiments with 1 km grid spacing, however, include only 5 years of each type of winter and in each climate. Here, we focus on

changes in the relationships with the progress of global warming in each type of winter (Fig. 8).

At all elevations, the winter temperature is lowest and highest in heavy and light snow-cover years, respectively (Figs. 8a–c). The winter temperature in heavy snow-cover years exceeds 0 °C below 500 m in the 1km_HIST experiment and below 1000 m in the 1km_4K experiment. The winter temperature is around 5 °C and 10 °C below 500 m in the 1km_HIST and 1km_4K experiments, respectively, in light snow-cover years. The winter temperature exceeds 0 °C at elevations between 500 and 1000 mASL in 1km_2K and even at elevations between 1000 and 1500 mASL in 1km_4K (Fig. 8c). The basic winter temperature is different among high, median, and light snow-cover years.

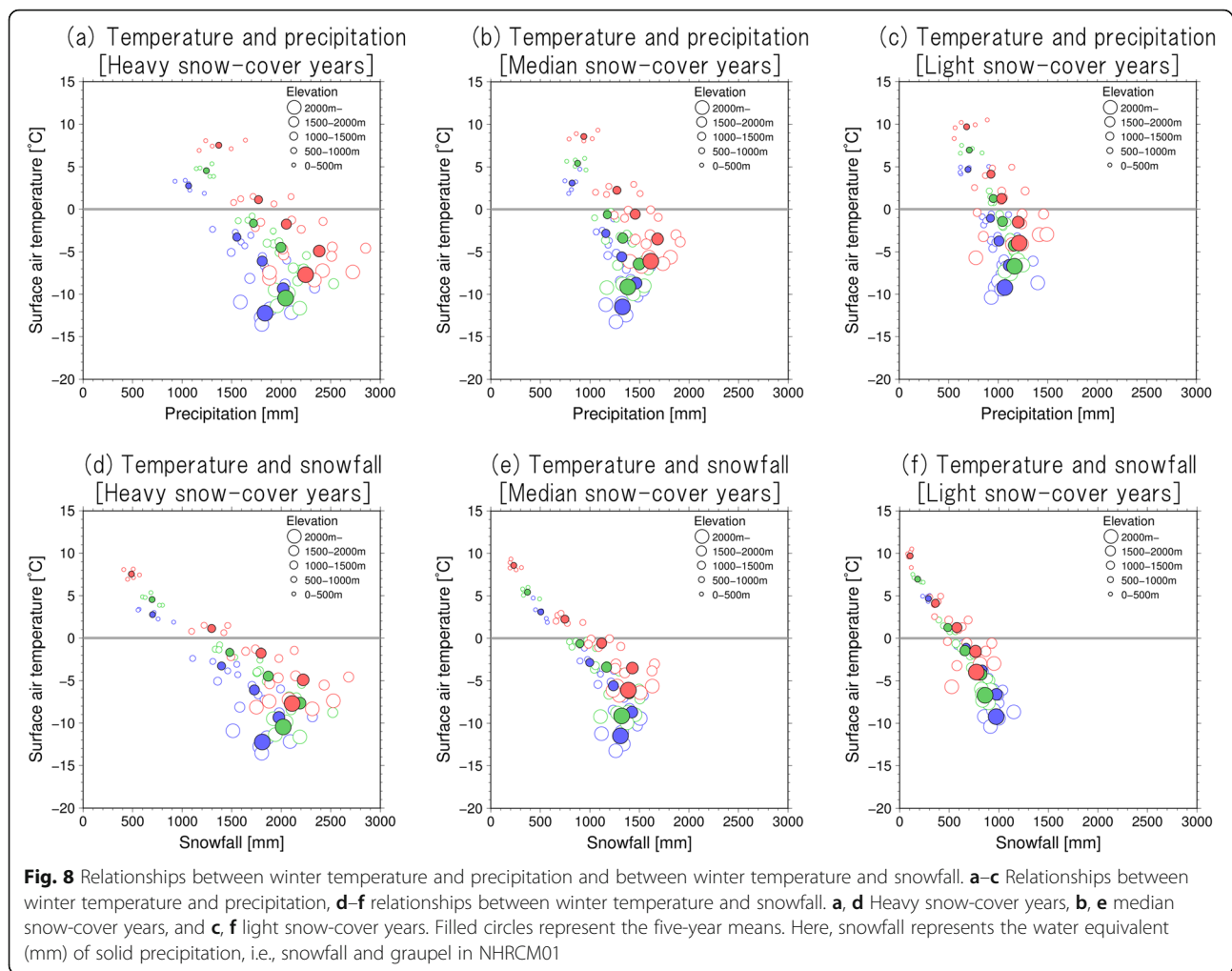In heavy snow-cover years, winter precipitation clearly increases with elevation (Fig. 8a), which is consistent

Fig. 8 Relationships between winter temperature and precipitation and between winter temperature and snowfall. **a–c** Relationships between winter temperature and precipitation, **d–f** relationships between winter temperature and snowfall. **a**, **d** Heavy snow-cover years, **b**, **e** median snow-cover years, and **c**, **f** light snow-cover years. Filled circles represent the five-year means. Here, snowfall represents the water equivalent (mm) of solid precipitation, i.e., snowfall and graupel in NHRCM01

with the findings of previous studies (e.g., Uno et al. 2014; Asaoka and Kominami 2013). Winter precipitation will increase with the progress of global warming at all elevations. In median snow-cover years, winter precipitation increases with elevation, while the increase ratio is smaller than that in heavy snow-cover years (Fig. 8b). The relationship between winter temperature and precipitation in light snow-cover years differs from those in heavy and median snow-cover years (Fig. 8c). The elevation dependency of winter precipitation is not clear, and global warming does not necessarily enhance winter precipitation in light snow-cover years.

Winter snowfall has a strong negative correlation with the winter mean temperature in all types of winter (Fig. 8d–f). On the other hand, the impacts of global warming on winter snowfall depend on the elevation and the type of winter. In heavy snow-cover years, snowfall decreases with the progress of global warming at low elevations below 500 mASL, where the winter temperature is 2–3 °C in the present climate (Fig. 8d). Winter snowfall totals do not change at middle

elevations—around 500–1500 mASL—where the winter temperature is from − 7 to − 2 °C in the present climate, in spite of global warming. At elevations above 1500 mASL, where winter temperatures are below − 7 °C in the present climate, winter snowfall obviously increases due to global warming. In median snow-cover years, winter snowfall decreases due to global warming below 1000 mASL (Fig. 8e). The decrease in snowfall is unclear at elevations higher than 1500 mASL. In light snow-cover years, winter snowfall decreases due to global warming not only at low elevations but also at high elevations (Fig. 8f). At elevations above 2000 mASL, winter precipitation in the 1km_4K experiment is comparable to that in the present climate, resulting in a reduction of snowfall, although the winter temperature is still around − 5 °C. Figure 8 indicates that future changes in snowfall depend on not only changes in winter temperatures but also changes in winter precipitation, which is strongly influenced by the type of winter. This result is a new finding as compared with those of previous studies.
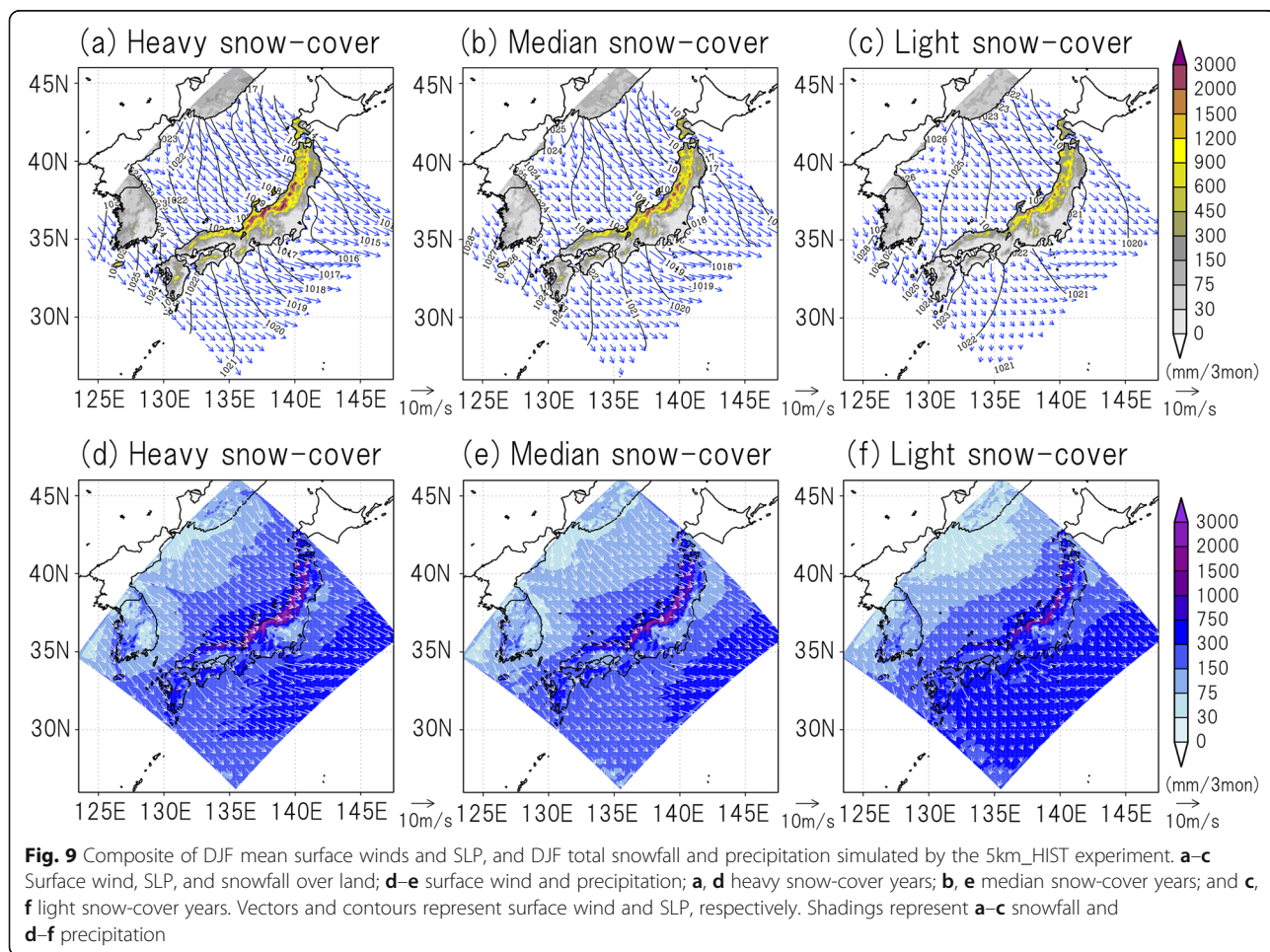
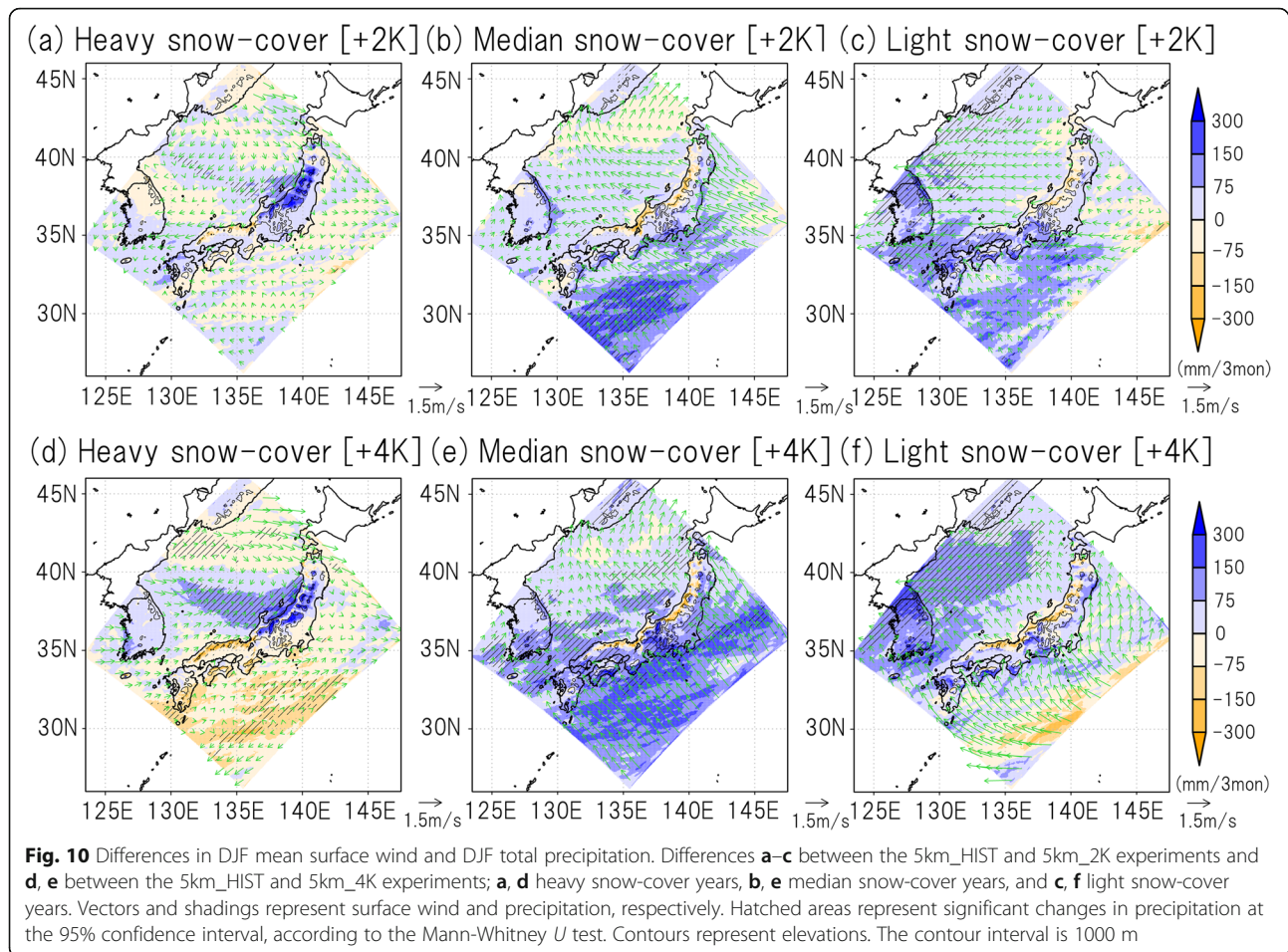## Characteristics of synoptic-scale atmospheric conditions

Future changes in snow cover and snowfall are caused by not only atmospheric warming and moistening, i.e., a thermo-dynamical effect, but also atmospheric circulation changes, i.e., a dynamical effect. Composite analyses are conducted by using d4PDF05 to discuss low-level atmospheric circulation changes and corresponding precipitation changes around Japan.

Figure 9a–c shows the DJF mean surface wind and sea level pressure (SLP) over the ocean and the DJF total water equivalent of falling snow and graupel over the Japanese archipelago in the 5km_HIST experiment. The typical SLP pattern in winter, i.e., higher pressure over west Japan and lower pressure over east Japan, appears, and the northwesterly prevails around Japan irrespective of the snow cover. The largest pressure gradient and strongest northwesterly in heavy snow-cover years reflect a strong or continuous cold surge during the winter (Fig. 9a). The smallest pressure gradient indicates that a weak northwesterly prevails in light snow-cover years (Fig. 9c).

Figure 10 shows differences in the surface wind over the ocean and precipitation between the 5km_HIST and 5km_2K experiments, and between the 5km_HIST and 5km_4K experiments. In heavy snow-cover years, the 5km_2K experiment simulates the increase in precipitation over the Sea of Japan's coast in eastern Japan (Fig. 10a). The northwesterly wind anomaly prevails over the northern part of the Sea of Japan. In median snow-cover years, on the other hand, precipitation decreases over the Sea of Japan's coast, and a southeasterly wind anomaly prevails around Japan (Fig. 9b). Precipitation increases over the coastal areas of the Pacific Ocean side and to the south of Japan. This means that the weakened winter monsoon reduces the precipitation over the coastal areas of the Sea of Japan and activates extratropical cyclones passing south of Japan, which brings precipitation over the coastal areas of the Pacific Ocean. The weakening of the winter monsoon due to global warming has been pointed out in previous studies (e.g., Hu et al. 2000; Kimoto 2005; Hori and Ueda 2006; Kawase et al. 2015). In addition, future changes in mid-winter storm tracks affect the winter precipitation in Japan. Inatsu and Kimoto (2005) examined the response of global warming to mid-winter

Fig. 9 Composite of DJF mean surface winds and SLP, and DJF total snowfall and precipitation simulated by the 5km_HIST experiment. **a**–**c** Surface wind, SLP, and snowfall over land; **d**–**e** surface wind and precipitation; **a**, **d** heavy snow-cover years; **b**, **e** median snow-cover years; and **c**, **f** light snow-cover years. Vectors and contours represent surface wind and SLP, respectively. Shadings represent **a**–**c** snowfall and **d**–**f** precipitation

Fig. 10 Differences in DJF mean surface wind and DJF total precipitation. Differences **a–c** between the 5km_HIST and 5km_2K experiments and **d**, **e** between the 5km_HIST and 5km_4K experiments; **a**, **d** heavy snow-cover years, **b**, **e** median snow-cover years, and **c**, **f** light snow-cover years. Vectors and shadings represent surface wind and precipitation, respectively. Hatched areas represent significant changes in precipitation at the 95% confidence interval, according to the Mann-Whitney *U* test. Contours represent elevations. The contour interval is 1000 m

storm tracks using a high-resolution atmospheric general circulation model and pointed out that global warming could make the storm tracks stronger in the western Pacific. Analyzing the reanalysis data from 1979/80 to 2010/11, Iwao et al. (2012) indicated that the frequency of explosively developing extratropical cyclones that originated southwest of Japan and passed south of Japan has been increasing east of Japan. Changes in the atmospheric circulation during median snow-cover years represent climatological changes in winter due to global warming. Over the mountainous areas of central Japan, the increase in precipitation due to activated extratropical cyclones is canceled out by the decrease in precipitation due to the weakened East Asian Winter Monsoon (Fig. 10b). In light snow-cover years, eastern and southeastern wind anomalies prevail around Japan, and precipitation increases from central Japan to western Japan (Fig. 10c).

On the other hand, the 5km_4K experiment shows recognizable changes in the surface wind and precipitation around Japan. In heavy snow-cover years, precipitation is enhanced over Japan's mountainous areas and over the central part of the Sea of Japan at a 95% confidence interval, according to the Mann-Whitney *U* test, while precipitation is inhibited over the western parts of Japan. The zonally enhanced precipitation band over the Sea of Japan corresponds to the enhancement of the JPCZ, where the precipitation is greater than that in the surrounding areas in 1km_HIST (Fig. 9a). Kawase et al. (2016) suggested that the enhancement of JPCZ due to global warming brought extremely heavy daily snowfall over the inland areas of the Sea of Japan side. Figure 10d indicates that not only extremely heavy daily snowfall events but also the winter mean atmospheric field shows the enhancement of JPCZ in heavy snow-cover years. Precipitation clearly decreases over the Sea of Japan coast in median snow-cover years, while precipitation increases over the Pacific Ocean side and mountainous areas of central Japan, which corresponds to the weakened winter monsoon (Fig. 10e). Changes during light snow-cover years also reflect the weakened winter monsoon, but the signals are smaller than those in median snow-cover years.

Our results indicate that the weakened winter monsoon effects changes in precipitation, including snowfall, in median and light snow-cover years, while the enhancement of the JPCZ brings increases in snowfall and snow cover in heavy snow-cover years in the high mountainous areas of central Japan, such as Japan's Northern Alps.

Conclusions

We conducted dynamical downscaling using NHRCM with 1 km and 5 km grid spacing from d4PDF 20 km NHRCM and investigated future changes in snowfall and snow cover over the high mountainous areas of central Japan. We picked up 5 years with heavy snow cover, 5 years with median snow cover, and 5 years with light snow cover over the Japanese Alps in three climates, i.e., the present climate and 2 K and 4 K warming climates relative to the pre-industrial period.

In heavy snow-cover years under 2 K and 4 K warming climates, the mid-winter snowfall amount is comparable to that in the present climate above 2000 mASL in the NN-Alps. Due to global warming, the amount of half-monthly snowfall becomes larger above 2000 mASL of the NN-Alps in mid-winter. The strengthened Japan-Sea Polar-airmass Convergence Zone (JPCZ) corresponds to the increase in snowfall during heavy snow-cover years, especially under a 4 K warming climate. Daily heavy snowfall is also strengthened under 4 K warming at high elevations. At lower elevations—below 500 m—the frequency of snowfall decreases in all ranges of snowfall intensity under a 4 K warming climate, while heavy snowfall increases under a 2 K warming climate.

On the other hand, a large reduction of snow cover is projected above 2000 mASL of the NN-Alps throughout the winter in light snow-cover years under a 4 K warming climate, which results from changes from snowfall to rainfall during the winter. These results indicate that the difference in mid-winter snow cover between heavy and light snow-cover years gets larger at high elevations of Japan's Northern Alps due to global warming. At low elevations, snow cover drastically decreases over the entire winter, and daily snowfall intensity is also weakened under both 2 K and 4 K warming climates.

Our simulations using NHRCM01 can resolve the complex Japanese mountains and evaluate the impact of global warming on years with heavy and light snow cover based on a large ensemble of climate simulations. However, we only analyzed 5 years of each snow-cover type under the present, 2K warming, and 4K warming climate conditions. Some of our results have large uncertainties. To more accurately evaluate future changes in snowfall over complex mountainous areas and elucidate the mechanisms in consideration of changes in atmospheric circulation, 10- to 20-year simulations are required using NHRCM01 in each climate.

Authors' contributions
HK proposed the topics, conducted the numerical simulations, and analyzed the output of the simulations. TY supported the analysis of the changes in snow cover in the mountainous areas. SS arranged the output of numerical simulations and supported the corresponding author in the construction of the manuscript. TH and MK provided the information about Japan's Northern Alps. TS and RI supported the conducting of the numerical simulations. MF created the boundary conditions of the 2 K warming experiments. AM, MN, and HS supported the establishing of the numerical design. All authors read and approved the final manuscript.

Author details
[1]Meteorological Research Institute, Japan Meteorological Agency, 1-1 Nagamine, Tsukuba 305-0052, Japan. [2]Department of Geophysics, Graduate School of Science, Tohoku University, 6-3 Aramaki Aza-Aoba, Aoba-ku, Sendai 980-8578, Japan. [3]Japan Agency for Marine-Earth Science and Technology, 3173-25 Showamachi, Kanazawa-ku, Yokohama 236-0001, Japan. [4]Japan Meteorological Business Support Center, 1-1 Nagamine, Tsukuba 305-0052, Japan. [5]Natural Environment Division, Nagano Environmental Conservation Research Institute, 2054-120 Kitago, Nagano 381-0075, Japan.

References

Aoki K, Watanabe K (2009) Measurements of atmospheric aerosol at Mt. Tateyama, Japan. Earozoru Kenkyu 24:112–116 (in Japanese with English abstract)

Aoyagi T, Seino N (2011) A square prism urban canopy scheme 671 for the NHM and its evaluation on summer conditions in the Tokyo metropolitan area, Japan. J Appl Meteorol Climatol 50:1476–1496

Asaoka Y, Kominami Y (2013) Incorporation of satellite-derived snow-cover area in spatial snowmelt modeling for a large area: determination of a gridded degree-day factor. Ann Glaciol 54:205–213

Brown RD, Mote P (2009) The response of Northern Hemisphere snow cover to a changing climate. J Clim 22:2124–2145

Fujita M, Mizuta R, Ishii M, Endo H, Sato T, Okada Y, Kawazoe S, Sugimoto S, Ishihara K, Watanabe S (2019) Precipitation changes in a climate with 2-K surface warming from large ensemble simulations by 60-km global and 20-km regional atmospheric models. Geophys Res Lett 46:435–442

Gula J, Peltier RW (2012) Dynamical downscaling over the Great Lakes basin of North America using the WRF regional climate model: the impact of the Great Lakes system on regional greenhouse warming. J Clim 25: 7723–7742

Gutmann ED, Rasmussen RM, Liu C, Ikeda K, Gochis DJ, Clark MP, Dudhia J, Thompson G (2012) A comparison of statistical and dynamical downscaling of winter precipitation over complex terrain. J Clim 25:262–281

Hara M, Yoshikane T, Kawase H, Kimura F (2008) Estimation of the impact of global warming on snow depth in Japan by the pseudo-global-warming method. HRL 2:61–64

Hirai M, Oh'izumi M (2004) Development of a new land-surface model for JMA-GSM. Proceedings of the 20th Conference on Weather Analysis and Forecasting/16th Conference on Numerical Weather Prediction, P2.22 [Available at https://ams.confex.com/ams/84Annual/techprogram/paper_68652.htm.]

Hori M E, Ueda H (2006) Impact of global warming on the East Asian winter monsoon as revealed by nine coupled atmosphere-ocean GCMs. Geophys Res Lett 33:L03713

Hu Z-Z, Bengtsson L, Arpe K (2000) Impact of the global warming on the Asian winter monsoon in a coupled GCM. J Geophys Res 105:4607–4624

Ikawa M, Mizuno H, Matsuo T, Murakami M, Yamada Y, Saito K (1991) Numerical modeling of the convective snow cloud over the Sea of Japan—precipitation mechanism and sensitivity to ice crystal nucleation rates. J Meteor Soc Japan 69:641–667

Ikeda K, Rasmussen R, Liu C, Gochis D, Yates D, Chen F, Tewari M, Barlage M, Dudhia J, Miller K, Arsenault K, Grubišić V, Thompson G, Guttman E (2010) Simulation of seasonal snowfall over Colorado. Atmos Res 97: 462–477

Imada Y, Watanabe M, Kawase H, Shiogama H, Arai M (2019) The July 2018 high temperature event in Japan could not have happened without human-induced global warming. SOLA 15A:8–12

Inatsu M, Kimoto M (2005) Two types of interannual variability of the mid-winter storm-tracks and their relationship to global warming. SOLA 1:61–64

Inoue S, Yokoyama K (1998) Estimation of snowfall, maximum snow depth and snowpack condition in Japan under global climate change. Seppyo 60:367–378 (in Japanese with English abstract)

Inoue S, Yokoyama K (2003) Estimates of snowfall depth, maximum snow depth, and snow pack environments under global warming in Japan from five sets of predicted data. J Agric Meteorol 59:227–236

Ishii Y, Suzuki K (2011) Regional characteristics of variation of snowfall in Japan. J Jpn Assoc Hydrol Sci 41:27–37 (in Japanese with English abstract)

Ishizaka M (2004) Climatic response of snow depth to recent warmer winter seasons in heavy-snowfall areas in Japan. Ann Glaciol 38:299–304

Ito R, Aoyagi T, Hori N, Oh'izumi M, Kawase H, Dairaku K, Seino N, Sasaki H (2018) Improvement of snow depth reproduction in Japanese urban areas by the inclusion of a snowpack scheme in the SPUC model. J Meteor Soc Japan 96: 511–534

Iwao K, Inatsu M, Kimoto M (2012) Recent changes in explosively developing extratropical cyclones over the winter Northwestern Pacific. J Clim 25: 7282–7296

Kain JS, Fritsch JM (1993) Convective parameterization for mesoscale models: the Kain-Fritsch scheme, in The Representation of Cumulus Convection in Numerical Models. Meteorological Monographs, Emanuel KA and Raymond DJ (eds.), chapter 24, pp. 165–170, Am Meteorol Soc, Boston

Katsuyama Y, Inatsu M, Nakamura K, Matoba S (2017) Global warming response of snowpack at mountain range in northern Japan estimated using multiple dynamically downscaled data. Cold Reg Sci and Technol 136:62–71

Kawase H, Hara M, Yoshikane T, Ishizaki NN, Uno F, Hatsushika H, Kimura F (2013) Altitude dependence of future snow cover changes over Central Japan evaluated by a regional climate model. J Geophys Res 118:12444–12457

Kawase H, Murata A, Mizuta R, Sasaki H, Nosaka M, Ishii M, Takayabu I (2016) Enhancement of heavy daily snowfall in central Japan due to global warming as projected by large ensemble of regional climate simulations. Climatic Change 139:265–278

Kawase H, Iida H, Aoki K, Shimada W, Nosaka M, Murata A, Sasaki H (2019a) Comparison of snow cover observations along the Tateyama-Kurobe Alpine route with snow cover simulations using the non-hydrostatic regional climate model (NHRCM) with different horizontal resolutions. J Geogr (Chigaku Zasshi) 128:77–92 (in Japanese with English abstract)

Kawase H, Imada Y, Sasaki H, Nakaegawa T, Murata A, Nosaka M, Takayabu I (2019b) Contribution of historical global warming to local-scale heavy precipitation in western Japan estimated by large ensemble high-resolution simulations. J Geophys Res 124:6093–6103

Kawase H, Suzuki C, Ishizaki NN, Uno F, Iida H, Aoki K (2015) Simulations of monthly variation in snowfall over complicated mountainous areas around Japan's Northern Alps. SOLA 11:138–143

Kawase H, Sasai T, Yamazaki T, Ito R, Dairaku K, Sugimoto S, Sasaki H, Murata A, Nosaka M (2018a) Characteristics of synoptic conditions for heavy snowfall in western to northeastern Japan analyzed by the 5-km regional climate ensemble experiments. J Meteor Soc Japan 96:161–178

Kawase H, Yamazaki A, Iida H, Aoki K, Sasaki H, Murata A, Nosaka M (2018b) Simulation of extremely small amounts of snow observed at high elevations over the Japanese Northern Alps in the 2015/16 winter. SOLA 14:39–45

Kawase H, Yoshikane T, Hara M, Fujita M, Ishizaki N, Hatsushika H, Kimura F (2012) Downscaling of snow cover changes in the late 20th century using a past climate simulation method over Central Japan. SOLA 8:61–64

Kimoto M (2005) Simulated change of the East Asian circulation under global warming scenario. Geophys Res Lett. https://doi.org/10.1029/2005GL023383

Kimura F, Kitoh A (2007) Downscaling by pseudo global warming method. The Final Report of the ICCAP:43–46

Kitagawa H (2000) Radiation processes. Separate volume of the annual report of numerical prediction division 46:16–31 (in Japanese)

Matsuura S, Matsuyama K, Asano S, Okamoto T, Takeuchi Y (2005) Fluctuation of the seasonal snowpack in a mountainous area of the heavy-snow district in the warm-temperate zone of Japan. J Glaciol 51:547–554

Mizuta R, Murata A, Ishii M, Shiogama H, Hibino K, Mori N, Arakawa O, Imada Y, Yoshida K, Aoyagi T, Kawase H, Mori M, Okada Y, Shimura T, Nagatomo T, Ikeda M, Endo H, Nosaka M, Arai M, Takahashi C, Tanaka K, Takemi T, Tachikawa Y, Temur K, Kamae Y, Watanabe M, Sasaki H, Kitoh A, Takayabu I, Nakakita E, Kimoto M (2017) Over 5000 years of ensemble future climate simulations by 60 km global and 20 km regional atmospheric models. Bull Amer Meteor Soc 98:1383–1398

Nakanishi M, Niino H (2004) An improved Mellor-Yamada level-3 model with condensation physics: its design and verification. Bound-Lay Meteor 112:1–31

Nakano M, Kato T, Hayashi S, Kanada S, Yamada Y, Kurihara K (2012) Development of a 5-km-mesh cloud-system-resolving regional climate model at the Meteorological Research Institute. J Meteor Soc Japan 90:339–350

Notaro M, Bennington V, Vavrus S (2015) Dynamically downscaled projections of lake-effect snow in the Great Lakes basin. J Clim 28:1661–1684

Ohba M, Sugimoto S (2019) Differences in climate change impacts between weather patterns: possible effects on spatial heterogeneous changes of future extreme rainfall. Clim Dyn 52:4177–4191

Raisanen J (2007) Warmer climate: less or more snow? Clim Dyn 30:307–319

Rasmussen R, Liu C, Ikeda K, Gochis D, Yates D, Chen F, Tewari M, Barlage M, Dudhia J, Yu W, Miller K (2011) High-resolution coupled climate runoff simulations of seasonal snowfall over Colorado: a process study of current and warmer climate. J Clim 24:3015–3048

Rasmussen R, Ikeda K, Liu C, Gochis D, Clark M, Dai A, Gutmann E, Dudhia J, Chen F, Barlage M, Yates D, Zhang G (2014) Climate change impacts on the water balance of the Colorado headwaters: High‐resolution regional climate model simulations. J Hydrometeorol 15:1091–1116

Sasai T, Kawase H, Kanno Y, Yamaguchi J, Sugimoto S, Yamazaki T, Sasaki H, Fujita M, Iwasaki T (2019) Future projection in extreme heavy snowfall event with 5-km large ensemble regional climate simulation. J Geophys Res. https://doi.org/10.1029/2019JD030781

Sasaki H, Kurihara K, Takayabu I, Uchiyama T (2008) Preliminary experiments of reproducing the present climate using the non-hydrostatic regional climate model. SOLA 4:25–28

Steger C, Kotlarski S, Jonas T, Schar C (2012) Alpine snow cover in a changing climate: a regional climate model perspective. Clim Dyn 41:735–754

Suzuki H (2006) Long-term changes in snowfall depth and snow cover depth in and around Niigata Prefecture from 1927 to 2005: analysis using data observed at railway stations. Tenki 53:185–196 (in Japanese with English abstract)

Takeuchi Y, Endo Y, Murakami S (2008) High correlation between winter precipitation and air temperature. Ann Glaciol 49:7–10

Uno F, Kawase H, Ishizaki NN, Yoshikane T, Hara M, Kimura F, Iyobe T, Kawashima K (2014) Analysis of regional difference in altitude dependence of snow depth using high resolve numerical experiments. SOLA 10:19–22

Yabu S, Murai S, Kitagawa H (2005) Clear sky radiation scheme. Separate Volume of the Annual Report of Numerical Prediction Division 51:53–64 (in Japanese)

Yamaguchi S, Abe O, Nakai S, Sato A (2011) Recent fluctuations of meteorological and snow conditions in Japanese mountains. Ann Glaciol 52:209–215

Publisher's Note